

Supplementary Materials for
**An Ancient CFTR Ortholog Informs Molecular Evolution in ABC
Transporters**

Guiying Cui, Jeong Hong, Yu-Wen Chung-Davidson, Daniel Infield, Xin Xu, Jindong Li, Luba Simhaev, Netaly Khazanov, Brandon Stauffer, Barry Imhoff, Kirsten Cottrill, J.E. Blalock, Weiming Li, Hanoch Senderowitz, Eric Sorscher, Nael A. McCarty, Amit Gaggar

Correspondence to: agaggar@uabmc.edu

This supplement includes:

Figs. S1 to S4

S1.

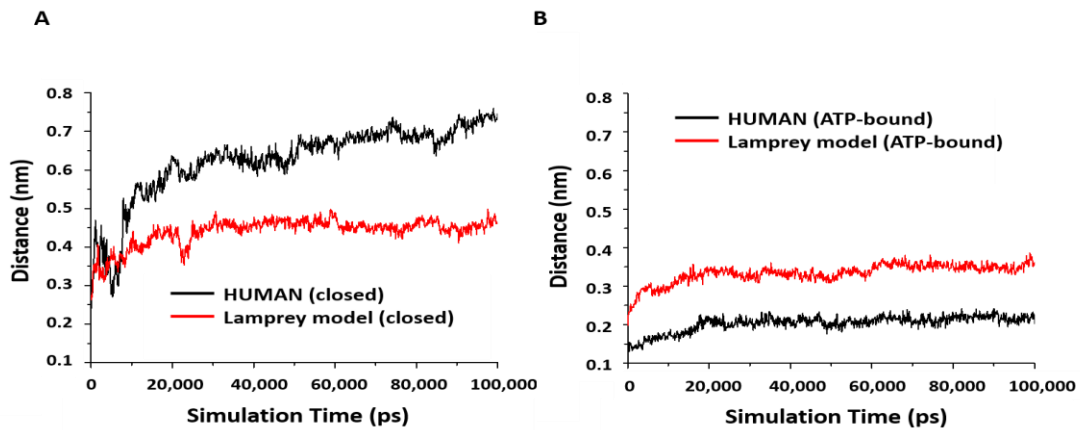


Figure S1: Lamprey CFTR adopts a more inward-facing conformation than human CFTR, related to Figure 1. Root mean square deviation (RMSD) of backbone atomic coordinates of hCFTR (in black) and Lp-CFTR (in red) conformations obtained from 100 ns MD simulations. **(A)** Closed hCFTR (5uak.pdb) and the corresponding Lp-CFTR model. **(B)** ATP-bound almost-open hCFTR (6msm.pdb) and the corresponding Lp-CFTR homology models.

S2.

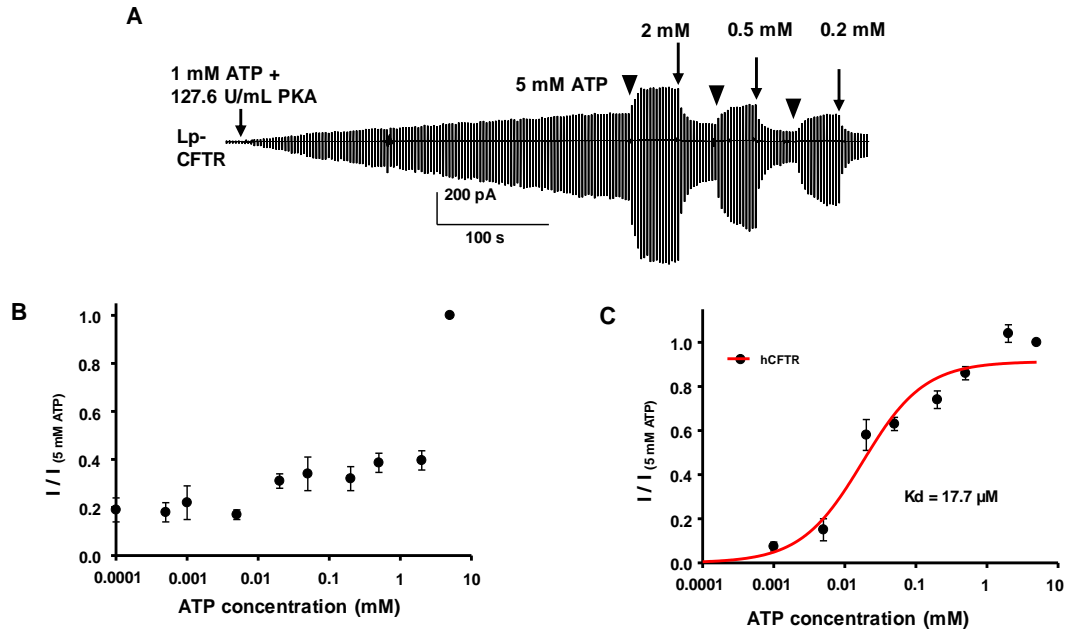


Figure S2. Lamprey CFTR exhibits reduced sensitivity to ATP concentration compared to human CFTR, related to Figure 2. **A.** Protocol for generation of dose-response curves for ATP-dependent activity. Lp-CFTR currents were measured in inside-out macropatches. After activation to steady state using PKA and 1 mM ATP, intracellular solution was changed to include 5 mM ATP (arrow heads) or lower ATP concentrations as indicated (arrows). Each test concentration was bracketed by 5 mM ATP. **B.** Dose-response curve for ATP-dependent activity of Lp-CFTR, normalized to current at 5 mM ATP. **C.** Dose-response curve for ATP-dependent activity of hCFTR, in experiments performed with the same protocol.

S3.

Rotifer ABCC4

Purple Sea Urchin ABCC4

Sea lamprey ABCC4

Sea lamprey CFTR

Dogfish shark CFTR

Zebrafish CFTR

Mouse CFTR

Human CFTR

vfyvpqepwiftaslrqnilfgkpyek-kkfneiikvccleed
 iaytaqqpwvfgtldrnilfgkkfdp-dkykealkvcalktd
 vayacqqpwvfpdtrqnilfgaayer-aryervvracsrlrkd
 lsfssqqpwiinasvqenitlglhldk-allwqvlrscglqee
 isyspqvpwimpgtikdniifglsyde-yrytsvvnacqleed
 isyssqtawimpgtirdnilfgltyde-yryksvkvacqleed
 vsfcsqfswimpgtikeniifgvsyde-yryksvkvacqlqqd
 isfcsqfswimpgtikeniifgvsyde-yryrsvikacqleed

Figure S3. Alignment of region of NBD1 surrounding F508 for invertebrate ABCC4 and vertebrate CFTR, related to Figure 1. ABCC4 from late invertebrate and early vertebrate species (rotifer, purple sea urchin, sea lamprey), and CFTR from vertebrates (dogfish shark, zebrafish, mouse, and human) are aligned and demonstrate an invariant phenylalanine (in red) except for Lp-CFTR.

S4.

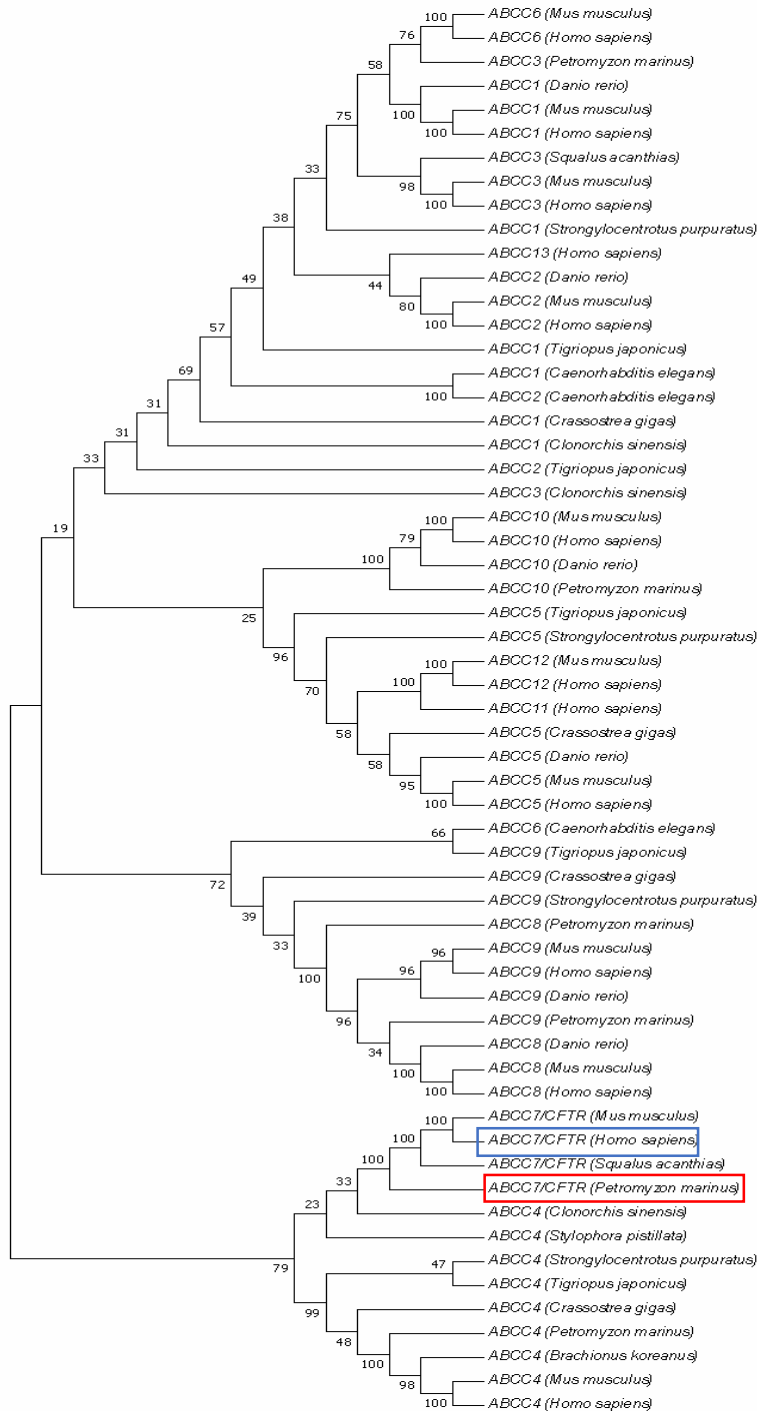


Figure S4. Maximum Parsimony Analysis of the Taxa, related to STAR Methods. The evolutionary history was inferred using the Maximum Parsimony (MP) method. The MP tree was obtained using the Subtree-Pruning-Regrafting (SPR) algorithm with search level 1 in which the initial trees were obtained by the random addition of sequences (10 replicates). The analysis involved 59 amino acid sequences. There were a total of 3423 positions in the final dataset. Evolutionary analyses were conducted in MEGA7. Lp-CFTR is noted in red box; hCFTR is noted in blue box.